Toxic effect of titanium dioxide nanoparticles on corneas *in vitro* and *in vivo*

Junxing Yang[1], Jianliang Liu[1], Ping Wang[1], Juanjuan Sun[1], Xiaohui Lv[1], Yumei Diao[1]

[1]Department of Ophthalmology, Weifang Medical University, Weifang 261042, Shandong Province, China

Correspondence to: Yumei Diao; **email:** diaoyumei2251@163.com, https://orcid.org/0000-0002-8565-2221

ABSTRACT

Titanium dioxide nanoparticles (TiO$_2$ NPs) are widely used in a variety of areas. However, TiO$_2$ NPs possess cytotoxicity which involves oxidative stress. Nuclear factor erythroid 2-related factor 2 (Nrf2) is a key molecule preventing cells from oxidative stress damage. In the current study, we explored the effect of Nrf2 signaling pathway in TiO$_2$ NPs-induced corneal endothelial cell injury. Firstly, we found TiO$_2$ NPs inhibited proliferation and damaged morphology and mitochondria of mouse primary corneal endothelial cells. Moreover, TiO$_2$ NPs-induced oxidative damage of mouse primary corneal endothelial cells was inhibited by antioxidant NAC by evaluating production of reactive oxygen species (ROS), malondialdehyde (MDA), and activities of superoxide dismutase (SOD) and glutathione peroxidase (GSH-Px). Next, flow cytometry analysis showed TiO$_2$ NPs promoted apoptosis and cell cycle G2/M phase arrest of mouse primary corneal endothelial cells. Further investigation suggested that Nrf2 signaling pathway activation and the downregulation of ZO-1, β-catenin and Na-K-ATPase were involved in TiO$_2$ NPs-induced mouse primary corneal endothelial cell injury. Our research highlighted the toxic effect of TiO$_2$ NPs on corneas *in vitro* and *in vivo*, providing an alternative insight into TiO$_2$ NPs-induced corneal endothelial cell injury.

INTRODUCTION

Nanomaterials are applied in food, medicine, cosmetics and other fields as the rapid development of nanotechnology [1, 2]. Recently, considerations have been given to the multifunction of titanium dioxide nanoparticles (TiO$_2$ NPs), a typical and widely applicable nanomaterial. However, it could not be ignored that the cytotoxic effect, immunotoxicity and inflammatory response of TiO$_2$ NPs exist when cells and organisms are exposed to TiO$_2$ NPs [3–5]. The toxic effect and the underlying mechanism are largely unclear.

In general, TiO$_2$ NPs could enter into the body through multiple approaches, like injection, inhalation and penetration [6], and cause damage of skin [7], respiratory system [8], brain [9], liver and other organs [10]. It should be concerned that NPs have been used as a topical ocular drug delivery system, the potential damage caused by NPs

cannot be ignored [11]. Notably, the NPs lead to a series of ophthalmic diseases such as corneal disorders [12] and retinal diseases [13], because of the direct contact between eyes and the NPs [14]. Accumulating evidence has reported that other types of NPs are also involved in the eye injury. Lee et al demonstrate that zinc oxide NPs-induced upregulation of Bax and heme oxygenase participates in the rabbit cornea cell injury, while silver NPs, TiO$_2$ NPs and silica oxide NPs have no effect on the expression of the two proteins [15]. A recent study shows that silver NPs destroy mitochondrial structure to aggravates cornea cell damage [16]. Therefore, the mechanisms of NPs-induced cytotoxicity vary according to the type of NPs. It has been demonstrated that TiO$_2$ NPs-induced oxidative stress contributes to the pathogenesis of damage of cells and organs [17]. The increased generation of reactive oxygen species (ROS) and the decreased antioxidant effect are major reasons to cause oxidative stress. When organisms are exposed to

TiO$_2$ NPs, the excessive ROS induce by TiO$_2$ NPs results in the inactivation of cell membrane proteins and damage of mitochondria and DNA, so as to generate toxic effects [17]. A recent research reported that three kinds of metal oxide NPs (TiO$_2$ NPs, zinc oxide NPs and polyvinylpyrrolidone capped zinc oxide NPs) were tested to select a preferable vehicle to be used in the treatment of glaucoma, and TiO$_2$ NPs were not suitable for further application because of the cytotoxicity of TiO$_2$ NPs [18]. Another study reported that TiO$_2$ NPs facilitated production of ROS and jeopardized the intracellular calcium homeostasis to inhibit proliferation of lens epithelial cells [19]. However, little is known about the role of TiO$_2$ NPs in corneal endothelial cells and its underlying mechanism.

In the present study, we investigated the toxic effect of TiO$_2$ NPs on corneal endothelial cells by using *in vitro* assays and *in vivo* experiments, highlighting a critical role of nuclear factor erythroid 2-related factor 2 (Nrf2)/antioxidant response element (ARE) signaling pathway in the pathogenesis of TiO$_2$ NPs-induced damage of corneal endothelial cells.

RESULTS

TiO$_2$ NPs boosted cell damage of corneal endothelial cells

First, TiO$_2$ NPs were observed by using transmission electron microscope (Figure 1A). Next, we treated corneal endothelial cells with different concentration of TiO$_2$ NPs for 24 h to examine cell viability. The results displayed that TiO$_2$ NPs decreased cell viability in a concentration-dependent manner (Figure 1B). Moreover, LDH content was significantly increased by TiO$_2$ NPs treatment (Figure 1C). The morphological analysis showed that the number of shrunken cells and dead cells was increased, and cell density was decreased when corneal endothelial cells were disposed to TiO$_2$ NPs (Figure 1D). To better illustrate the oxidative damage of corneal endothelial cells, we took H$_2$O$_2$ treatment as the positive control (Figure 1C). In addition, we detected cell damage from a more microscopic point of view by evaluating mitochondrial membrane potential and found TiO$_2$ NPs decreased red fluorescence intensity and increased green fluorescence intensity (Figure 1E), suggesting that TiO$_2$ NPs led to mitochondrial damage.

Oxidative damage of TiO$_2$ NPs to corneal endothelial cells

To further determine the oxidative damage of TiO$_2$ NPs on corneal endothelial cells, we detected the following indicators and H$_2$O$_2$ treatment was used as the positive control. DCFH-DA is widely used to detect intracellular

ROS [20]. We observed that TiO$_2$ NPs augmented fluorescence intensity (Figure 2A), indicating the elevation of ROS generation. Meanwhile, NAC, a potent scavenger of ROS, could weaken the increased fluorescence intensity induced by TiO$_2$ NPs (Figure 2A). In addition, TiO$_2$ NPs increased MDA content in corneal endothelial cells, and NAC could antagonize the harmful role of TiO$_2$ NPs (Figure 2B). We also found that the activity of either SOD or GSH-Px, two major enzymes acting as antioxidants, was decreased by TiO$_2$ NPs in corneal endothelial cells, which was partially reversed by NAC treatment (Figure 2C and 2D).

TiO$_2$ NPs caused apoptosis and cell cycle arrest of corneal endothelial cells

Apoptosis and cell cycle arrest are two biological indicators that inhibit cell proliferation. The flow cytometry analysis revealed that TiO$_2$ NPs promoted apoptotic rate of corneal endothelial cells in a concentration-dependent manner (Figure 3A). Additionally, as was shown in Figure 3B, the proportion of cell cycle G2/M phase arrest was increased by TiO$_2$ NPs treatment in a concentration-dependent manner (Figure 3B).

TiO$_2$ NPs activated Nrf2/ARE signaling pathway in corneal endothelial cells

Nrf2/ARE signaling pathway is a key component to exert an antioxidant role [21]. We found that TiO$_2$ NPs treatment significantly upregulated the mRNA level of Nrf2 in corneal endothelial cells (Figure 4A). Additionally, Nrf2 overexpression plasmid was transfected into corneal endothelial cells as the positive control. Further experiments revealed that either TiO$_2$ NPs treatment or Nrf2 overexpression could dramatically increase the mRNA level of Nrf2 downstream molecules HO1, NQO1 and γ-GCS (Figure 4B–4D). Conversely, the mRNA level of Keap1 was decreased by TiO$_2$ NPs treatment and Nrf2 overexpression (Figure 4E). In addition, we found that NAC could partially antagonize TiO$_2$ NPs-induced aberrant mRNA levels of Nrf2, HO1, NQO1, γ-GCS and Keap1 (Figure 4A–4E). Western blot analysis by detecting the protein levels of Nrf2 and Keap1 showed the similar results as RT-PCR did in corneal endothelial cells (Figure 4F). In parallel, H$_2$O$_2$ treatment displayed the similar results as TiO$_2$ NPs did (Figure 4A–4F). These findings suggested that TiO$_2$ NPs activated Nrf2-related signaling pathway in corneal endothelial cells.

Regulation of functional proteins by TiO$_2$ NPs in corneal endothelial cells

Next, we investigated the role of TiO$_2$ NPs in regulation of cell-cell contact-related proteins. The

immunofluorescence analysis showed that TiO$_2$ NPs treatment reduced the expression of ZO-1 and Na-K-ATPase in corneal endothelial cells (Figure 5A and 5B). Moreover, we found the expression of β-catenin in nucleus of corneal endothelial cells was significantly decreased by TiO$_2$ NPs treatment (Figure 5C).

TiO$_2$ NPs damaged corneas *in vivo*

Finally, we performed *in vivo* experiments to evaluate the harmful role of TiO$_2$ NPs. After exposure to TiO$_2$ NPs, the corneas displayed decreased transparency *in vivo* (Figure 6A). Histologically, the corneas were
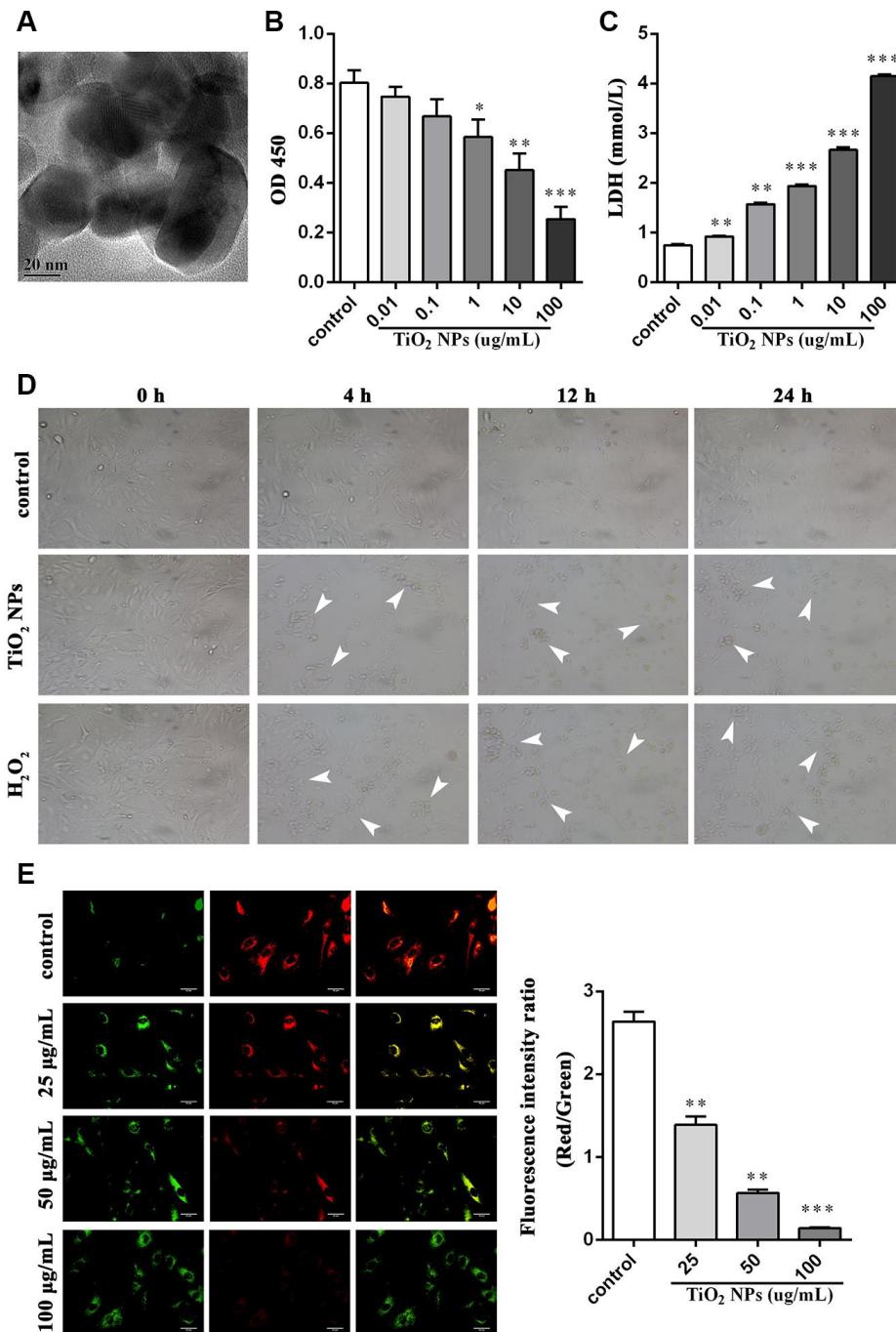

Figure 1. TiO$_2$ NPs boosted cell damage of corneal endothelial cells. (**A**) Detection of shape and size of TiO$_2$ NPs by TEM, bar = 20 nm. (**B**) Cell viability of TiO$_2$ NPs-treated primary endothelial cells. (**C**) Measurement of LDH content in TiO$_2$ NPs-treated primary endothelial cells. (**D**) Morphological analysis of TiO$_2$ NPs-treated primary endothelial cells by inverted microscope, bar = 50 μm. (**E**) Mitochondrial membrane potential of TiO$_2$ NPs-treated primary endothelial cells by using JC-1, bar = 30 μm. *P<0.05, **P<0.01, ***P<0.001.

infiltrated with a large number of inflammatory cells (Figure 6B). The *in situ* TUNEL staining analysis showed that the number of TUNEL-positive cells was clearly increased in cornea of TiO_2 NPs-treated mice (Figure 6C), indicating that TiO_2 NPs promoted apoptosis of corneal cells. Moreover, MDA content was significantly increased and the activities of SOD and GSH-Px were remarkably decreased by TiO_2 NPs in plasm of mice (Figure 6D-6F), which was in line with the results of *in vitro* assays (Figure 2B-2D). The *in vivo* experiments suggested that TiO_2 NPs not only caused cornea damage, but also resulted in potentially systemic injury.

DISCUSSION

TiO_2 NPs, a kind of newly inorganic chemical material, have been widely used in a variety of fields involving chemistry, physics, biology and medicine. However, research on toxicity of TiO_2 NPs has not kept pace with its application. In the present study, we found TiO_2 NPs damaged morphology and cell viability of corneal
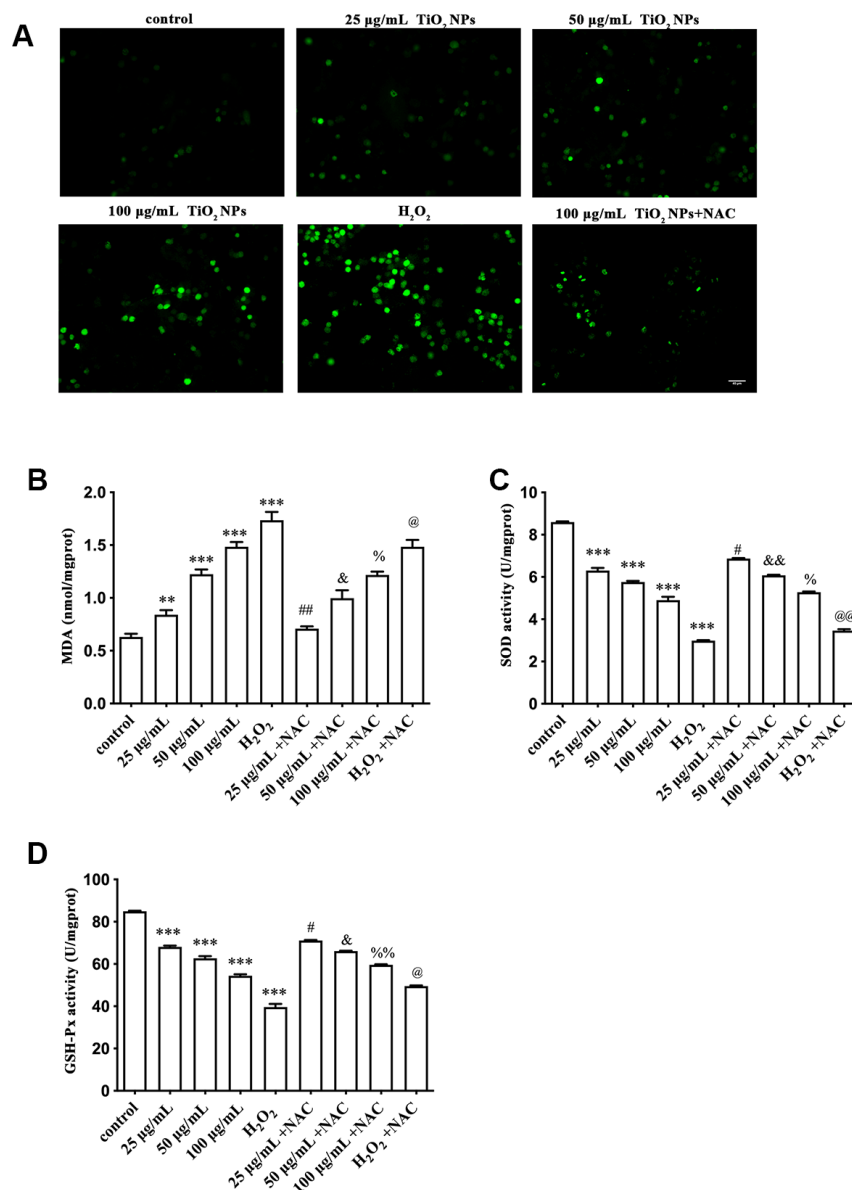

Figure 2. Oxidative damage of TiO₂ NPs to corneal endothelial cells. (**A**) Intracellular ROS of corneal endothelial cells with indicated treatment, bar = 40 μm. Detection of MDA content (**B**), SOD activity (**C**) and GSH-Px activity (**D**) in primary corneal endothelial cells with indicated treatment. **P<0.01 vs. control group, ***P<0.001 vs. control group, #P<0.05 vs. 25 μg/mL group, ##P<0.01 vs. 25 μg/mL group, &P<0.05 vs. 50 μg/mL group, &&P<0.01 vs. 50 μg/mL group, %P<0.05 vs. 100 μg/mL group, %%P<0.01 vs. H₂O₂ group, @P<0.05 vs. 50 μg/mL group, @@P<0.01 vs. H₂O₂ group.

endothelial cells. Moreover, biochemical indicators revealed that antioxidant NAC restrained TiO_2 NPs-induce oxidative injury by evaluating ROS generation, MDA content, and the activities of antioxidases SOD and GSH-Px.

Currently, oxidative stress is the dominating factor that induces toxic effects of TiO_2 NPs to organisms [17, 22, 23]. ROS are intermediates and end products during redox process, and ROS generation and elimination display a dynamic equilibrium state [24]. It has been reported that moderate ROS production is necessary to maintain normal physiological activities of cells and organisms [25]. Therefore, ROS overproduction could contribute to pathophysiological foundation of multiple diseases. MDA, a kind of degradation product formed in the process of lipid peroxidation, is a common indicator to reflect oxidative damage of cells [26]. We found that ROS generation in TiO_2 NPs-treated corneal endothelial cells was accompanied by the increased MDA content.
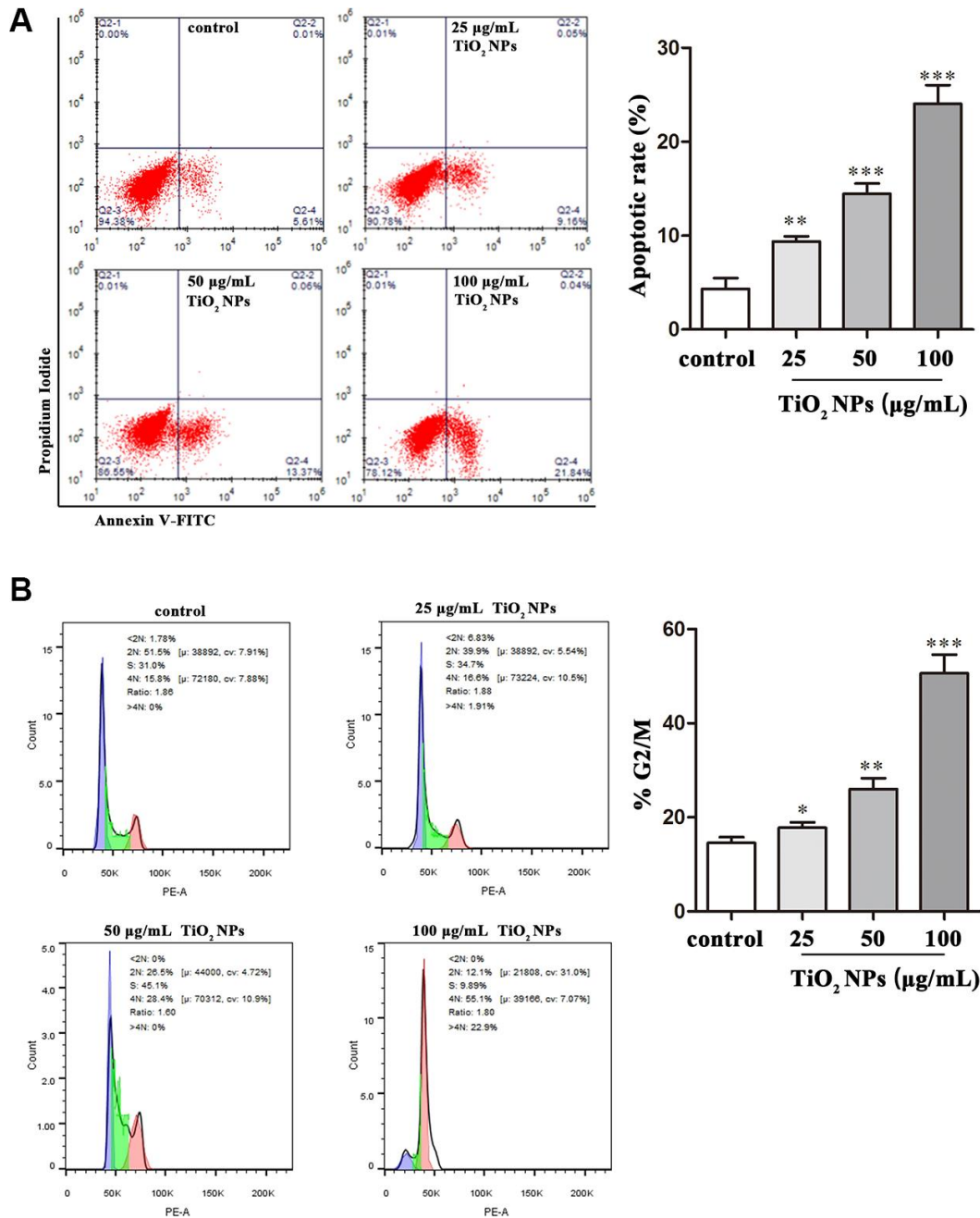

Figure 3. TiO_2 NPs caused apoptosis and cell cycle arrest of corneal endothelial cells. Apoptosis analysis (**A**) and cell cycle analysis (**B**) of TiO_2 NPs-treated primary corneal endothelial cells by using flow cytometry. $^{*}P<0.05$, $^{**}P<0.01$, $^{***}P<0.001$.

Moreover, TiO₂ NPs restrained SOD activity and GSH-Px activity of corneal endothelial cells. SOD and GSH-Px are two major enzymes that play a crucial role in anti-oxidative damage [27]. *In vivo* experiments suggested that TiO₂ NPs could reduce the activities of SOD and GSH-Px in cortex and hippocampus of mice [28]. Abbasi-Oshaghi et al reported that TiO₂ NPs promoted activation of NLRP3 inflammation and ROS generation, and reduced expression and activities of a variety of antioxidases in liver [29]. In addition, we found that TiO₂ NPs led to cell cycle G2/M phase arrest of primary corneal endothelial cells. It has been widely reported that ROS induces DNA damage by oxidized modification of bases and breaking DNA strands [30]. DNA damage contributes to cell cycle arrest to provide sufficient time for repairing, thus avoiding the damage
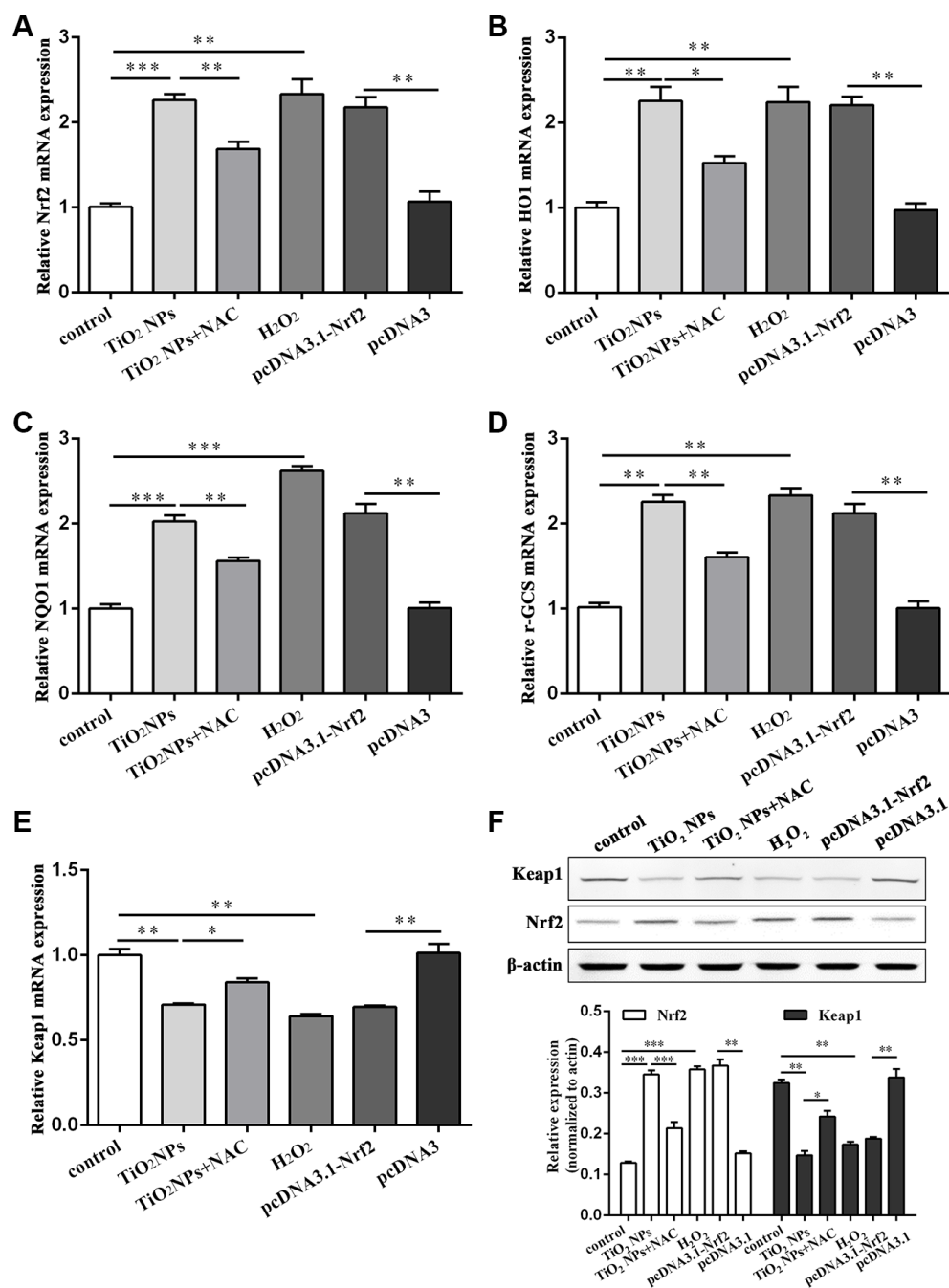

Figure 4. TiO₂ NPs activated Nrf2/ARE signaling pathway in corneal endothelial cells. The mRNA level of Nrf2 (**A**), HO1 (**B**), NQO1 (**C**), γ-GCS (**D**), Keap1 (**E**) in primary corneal endothelial cells with indicated treatment. (**F**) Protein level of Keap1 and Nrf2 in primary corneal endothelial cells with indicated treatment. $^{*}P<0.05$, $^{**}P<0.01$, $^{***}P<0.001$.

to be inherited to daughter cells; when the damage could not be efficiently repaired, cell apoptosis occurs [31, 32]. Kansara et al demonstrated that TiO$_2$ NPs-mediated upregulation of CdC2 and downregulation of Cyclin B1 were involved in cell cycle G2/M phase arrest and apoptosis of human alveolar cells [8]. We also found that TiO$_2$ NPs-induced apoptosis of corneal endothelial cells was accompanied by the remarkably increased proportion of cell cycle G2/M phase.

Although the toxic effect of TiO$_2$ NPs has been extensively investigated, the exact underlying mechanism of TiO$_2$ NPs-related cell injury is still unclear. A recent research suggested that TGF-β1/Smad3/p38 signaling
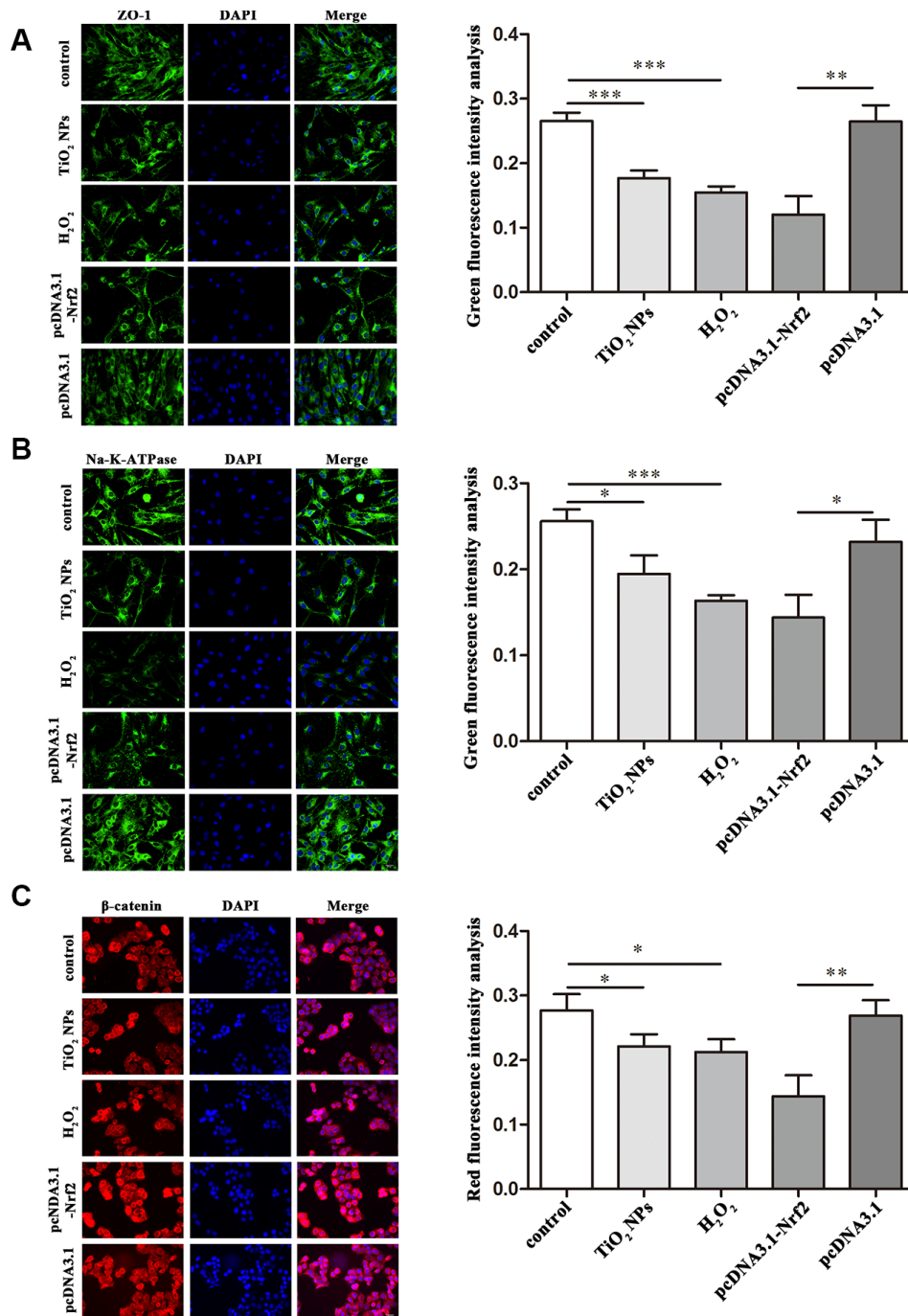

Figure 5. Regulation of functional proteins by TiO$_2$ NPs in corneal endothelial cells. Immunofluorescence analysis of the expression of ZO-1 (**A**), Na-K-ATPase (**B**) and β-catenin (**C**) in primary corneal endothelial cells with TiO$_2$ NPs treatment, H$_2$O$_2$ treatment or Nrf2 overexpression. bar = 20 μm. *P<0.05, **P<0.01, ***P<0.001.

pathway participated in TiO$_2$ NPs-induced renal cell damage [33]. In breast cancer cells, TiO$_2$ NPs inactivated EGFR to inhibit activation of the downstream signaling pathway AKT and ERK, reducing cell adhesion and facilitating cell apoptosis [34]. In our study, we found Nrf2/ARE signaling pathway might contribute to the pathogenesis of TiO$_2$ NPs-induced corneal endothelial cell injury. Normally, Nrf2 is bonded and inactivated by Keap1 in cytoplasm; when stimuli enable oxidative stress in cells, the negative regulation of Keap1 on Nrf2 is thus inhibited,

and Nrf2 transfers to nucleus to interact with ARE so as to facilitate the expression of the downstream molecules [21]. Nrf2 is a key transcription factor that participates in anti-oxidative stress damage. Our findings indicated that TiO$_2$ NPs promoted the expression of Nrf2 and target genes of Nrf2/ARE signaling pathway (HO1, NQO1 and γ-GCS). HO1, the inducible type of heme oxygenase, is a kind of rate-limiting enzyme that could degrade abnormal hemoglobin in blood [35]. NQO1 belongs to phase II enzymes, providing a protective role in oxidative damage. It has been verified that both HO1
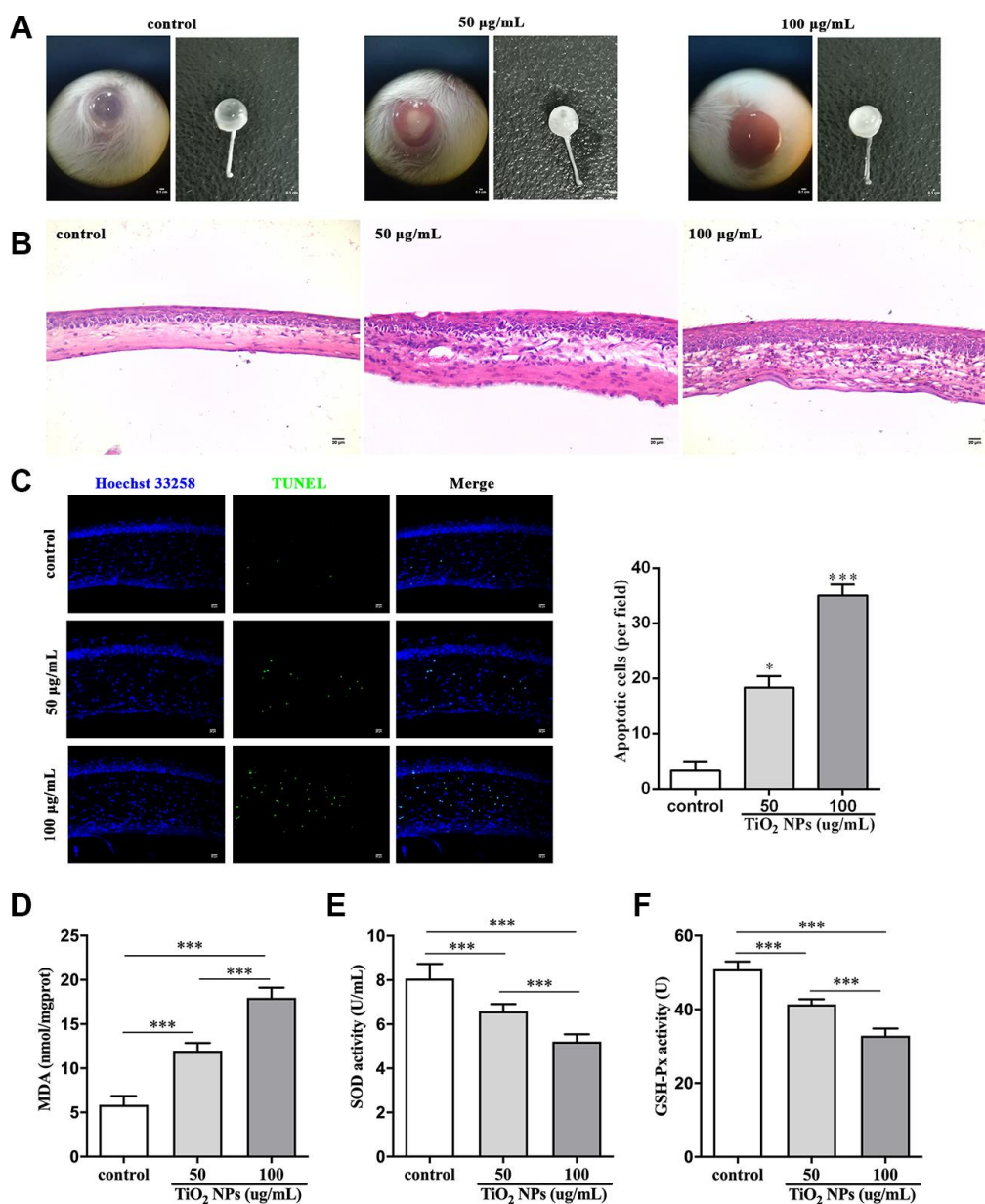

Figure 6. TiO$_2$ NPs damaged corneas *in vivo*. (**A**) Images of eyeballs after indicated treatment *in vivo*, bar = 0.1 cm. (**B**) Histological observation of corneas with HE staining after TiO$_2$ NPs treatment, bar = 20 μm. (**C**) Detection of apoptotic cells in cornea of TiO$_2$ NPs-treated mice with TUNEL staining, bar = 20 μm. Measurement of MDA content (**D**), SOD activity (**E**) and GSH-Px activity (**F**) *in vivo*. *P<0.05, ***P<0.001.

and NQO1 are involved in corneal endothelial cell injury induced by physical and chemical factors [36, 37]. We further identified γ-GCS as a downstream molecule of Nrf2 in TiO$_2$ NPs-induced oxidative damage of corneal endothelial cells.

Additionally, we found downregulation of ZO-1, Na-K-ATPase and β-catenin in TiO$_2$ NPs-treated corneal endothelial cells. ZO-1 is tight junction protein that is involved in signal transduction at cell-cell junctions, which is also a key mediator for cell proliferation [38]. Na-K-ATPase is an enzyme that drives sodium and potassium to maintain cell homeostasis [39]. A recent study revealed that Roof plate-specific spondin 1-induced proliferation of corneal endothelial cells was associated with the two functional proteins ZO-1 and Na-K-ATPase, and nuclear translocation of β-catenin boosted the expression of proliferation-associated Cyclins [40]. Hong et al demonstrated that TiO$_2$ NPs downregulated the protein level of Wnt3a and β-catenin, and inactivated Wnt3a/β-catenin signaling pathway to block development of neurons [41]. Combined with these results, our research suggested that downregulation of ZO-1, Na-K-ATPase and β-catenin might contribute to the decreased proliferation of TiO$_2$ NPs-treated corneal endothelial cells. Taken together, our findings uncovered the crucial role of Nrf2/ARE signaling pathway and functional proteins ZO-1, Na-K-ATPase and β-catenin in TiO$_2$ NPs-induced corneal endothelial cell injury, providing an alternative insight into the toxic effects of TiO$_2$ NPs.

MATERIALS AND METHODS

Shape and size of TiO$_2$ NPs

TiO$_2$ NPs powder (Sigma-Aldrich, Germany) was heated at 120° C for 2 h and dissolved into sterile distilled water. After cooling naturally, the TiO$_2$ NPs solution was stored at 4° C. In addition, the TiO$_2$ NPs solution was vibrated by ultrasonic oscillation for 30 min before the assays. Observation of TiO$_2$ NPs was detected by transmission electron microscope (TEM, Hitachi, Japan).

Animal preparation

BALB/c mice (7-8-week-old) were purchased from Animal Laboratory Center of Weifang Medical University and raised in cages at 20° C ~ 24° C. The mice were free to obtain food and water and housed in the 12-hour light/dark cycle. The animal experiments were authorized by Animal Care and Use Committee of Weifang Medical University, and the procedures were act in accordance with the requests of Animal Care and Use Committee of Weifang Medical University. The mice

were randomly divided into three groups: control group (n=15), 50 μg/mL TiO$_2$ NPs group (n=15) and 100 μg/mL TiO$_2$ NPs group (n=15). Eyes of mice in control group were exposed to distilled water and eyes of mice in the other two groups were exposed to different concentration of TiO$_2$ NPs solution. All mice were treated once a day for one week, followed by being narcotized with 5% chloral hydrate to remove eyeballs.

Hematoxylin-eosin (HE) staining

The procedure of HE staining for corneas was processed as previously shown [42] with a slight modification. In brief, the isolated tissues were fixed with 4% paraformaldehyde followed by dehydration and being stained by using Hematoxylin and Eosin Staining Kit (Beyotime, China). The images were observed and obtained with microscopy (Olympus, Japan).

In situ TUNEL staining

The isolated corneas were incubated with TUNEL solution (Beyotime, China) to detect apoptosis *in situ*, and nuclei were stained with Hoechst 33285 (Beyotime, China). The detailed method was carried out in accordance with the manufacturer's guidelines.

Isolation of mouse primary corneal endothelial cells

BALB/c mice, aged 4-5 weeks, were obtained from the Animal Experimental Center of Weifang Medical University. The procedures of isolation of mouse corneal buttons were conducted as previously reported [43] with a modification. Briefly, eyes of mice were carefully removed after mice were killed, followed by being washed with phosphate-buffered saline (PBS). Corneal buttons were isolated and washed with PBS. The corneal endothelium was digested by 0.25% Trypsin-EDTA (Thermo Fisher Scientific, USA) at 37° C for 20 min. The corneal endothelial cells were harvested and cultured in M199 Medium (Thermo Fisher Scientific, USA) with 10% fetal bovine serum (Gibco, USA), followed by being subcultured at 1:3 split and cultured in Incubator (Thermo Fisher Scientific, USA) at 37° C with 5% CO2.

Detection of cell viability

Cell viability was evaluated by using Cell Counting Kit-8 (CCK8, Beyotime, China) according to the manufacturer's instruction. Cells were seeded in a 96-well plate at a density of 8000 cells per well. After 24 h, the cells were treated with different concentration of TiO$_2$ NPs for 24 h. 110 μL fresh medium containing 10 μL reagents was replaced in each well at 37° C for 2 h. The value of optical density (OD) was detected by Microplate Reader (Bio-Rad, USA) at 450 nm.

Cytotoxicity assay

The content of lactate dehydrogenase (LDH) was detected by using LDH Cytotoxicity Assay Kit (Beyotime, China) to evaluate the cytotoxicity of TiO_2 NPs according to the manufacturer's guidelines. In brief, the cells were seeded in a 96-well plate at a density of 8000 cells per well. After 24 h, the cells were treated with different concentration of TiO_2 NPs for 24 h. After centrifuging, 120 μL supernatant in each well was transferred into a new 96-well plate followed by adding the reagents, and the OD value was detected by Microplate Reader (Bio-Rad, USA) at 490 nm.

Morphological analysis of TiO_2 NPs-treated corneal endothelial cells

The primary corneal endothelial cells were disposed to either 25 μg/mL TiO_2 NPs or 1.0 mM H_2O_2 for indicated time, followed by being observed by inverted microscope (Olympus, Japan). The magnification was 40×10.

Measurement of mitochondrial membrane potential

Mitochondrial membrane potential assay kit with JC-1 (Beyotime, China) was utilized to determine mitochondrial membrane potential of TiO_2 NPs-treated corneal endothelial cells in accordance with the manufacturer's instrument. JC-1 aggregates were represented as red fluorescence and JC-1 monomers were indicated as green fluorescence.

ROS detection

The intracellular ROS was determined by using ROS Assay Kit (Beyotime, China) according to the manufacturer's guidelines. The cells were seeded in a 6-well plate and treated with different concentration of TiO_2 NPs in the presence of NAC (10 mM, Beyotime, China). Next, 1.5 mL diluted DCFH-DA was added into each well for 20 min. Cells were washed with serum-free medium for three times and observed by fluorescence microscope (Olympus, Japan). After that, the cells were harvested and analyzed by BeamCyte (China).

Measurement of malondialdehyde (MDA) content, superoxide dismutase (SOD) activity and glutathione peroxidase (GSH-Px) activity

MDA content, SOD activity and GSH-Px activity in primary endothelial cells and plasma were detected with Malondialdehyde Assay Kit (JianchengBio, China), Superoxide Dismutase Assay Kit (JianchengBio, China)

and Glutathione Peroxidase Assay Kit (JianchengBio, China) in accordance with the manufacturer's guidelines.

Measurement of apoptosis

Apoptotic cells were detected by using Annexin V-FITC/PI Apoptosis Detection Kit (Beyotime, China). Briefly, cells were seeded into a 6-well plate and treated with different concentration of TiO_2 NPs for 24 h. Next, the cells were washed with PBS for three times and stained with 5 μL Annexin V-FITC for 5 min in the dark at room temperature, followed by being added with 10 μL Propidium Iodide (PI) for 15 min. Next, the samples were detected with BeamCyte (China) and analyzed with CytoSYS 1.0 software. Apoptotic cells were represented as the Annexin V (+)/PI (-) cells.

Cell cycle analysis

Cell Cycle and Apoptosis Kit (Beyotime, China) was utilized to detect cell cycle. Briefly, cells were washed with pre-cooled PBS and fixed with 70% ethanol for 24 h overnight. After that, 0.2% Triton X-100 was added into the cell solution, followed by re-suspended with 100 μg/mL RAase A for 30 min. Next, 10 μL PI solution was added for staining at 37° C in the dark. BeamCyte (China) was used to analyze the results.

Cell transfection

The Nrf2 overexpression plasmid pcDNA3.1-Nrf2 was synthesized from Sangon Biotech (China). Cell transfection was performed by using Lipofectamine 3000 (Invitrogen, USA) in accordance with the manufacturer's guidelines.

Quantitative real time-polymerase chain reaction (qRT-PCR)

RNA was extracted by using TRIzol (Ambion, Germany). cDNA was acquired from the extracted RNA, and qRT-PCR was carried out by using SYBR Premix Ex Taq II Kit (Takara, Japan), and the expression level was calculated by using $2^{-\Delta\Delta CT}$ methods. The primers were synthesized from Sangon Biotech (China) and shown in Table 1.

Western blot

RIPA (Beyotime, China) was used to lyse the cells, and protein concentration was detected with BCA Kit (Beyotime, China). The protein was separated by SDS-PAGE gels (Beyotime, China) and transferred to the PVDF membrane (Millipore, USA). After being blocked with 5% BSA, the membranes were incubated

Table 1. The sequences of primers.

Gene	Sequence (5'-3')
Nrf2	Forward: TGGTTAAGATGGTCCACACGG
	Reverse: GCTGGAAGCTCGGTGTTAGT
HO1	Forward: CACAGATGGCGTCACTTCGT
	Reverse: GGGCGCTTTTGTCTGTACC
NQO1	Forward: TGGCCAATGGTTCACCTACC
	Reverse: TTCACCCGTCCTGTTTGGAT
γ-GCS	Forward: AGGCGATCTCTCTCCACTGT
	Reverse: ATGCCAGTCTCACCTTTCGG
Keap1	Forward: GTTGCCATCCGGAGAGTTGT
	Reverse: CAGTGTGTGGCCTGTGTGAC
GAPDH	Forward: TGAAATGTGCACGCACCAAG
	Reverse: GGGAAGCAGCATTCAGGTCT

with primary antibodies (Rabbit polyclonal to Keap1, Abcam, USA; Rabbit monoclonal to Nrf2, Abcam, USA; Mouse monoclonal to beta Actin-Loading Control, Abcam, USA) overnight at 4° C. After being washed, the membranes were incubation with secondary antibodies (Beyotime, China). ChemDoc™ XRS+ System (Bio-Rad, USA) was utilized to evaluate the protein bands.

Immunofluorescence analysis

Primary corneal endothelial cells were fixed with 4% paraformaldehyde for 10 min. After being washed, cells were incubated with 0.1% Triton X-100 for 10 min at room temperature. Next, cells were washed and blocked with normal goat serum for 30 min followed by primary antibodies (Rabbit monoclonal to ZO-1 tight junction protein, Abcam, USA; Rabbit monoclonal to Sodium Potassium ATPase-Plasma Membrane Marker, Abcam, USA; Rabbit monoclonal to beta Catenin, Abcam, USA) overnight at 4° C. After being washed, the cells were incubated with secondary antibodies (Goat anti-rabbit IgG-Alexa Fluor 488 Conjugated, ZhuangzhiBIO, China; Goat anti-rabbit IgG-Cy3 Conjugated, ZhuangzhiBIO, China) for 1 h at room temperature in the dark, followed by being incubated with DAPI Staining Solution (Beyotime, China) for 10 min. Fluorescence analysis was performed with laser scanning confocal microscopy (Olympus, Japan).

Statistical analysis

All the data in this work were represented as mean ± standard deviation (SD) with three independent experiments, and analyzed with non-parametric t tests by using the GraphPad Prism 5.0 Software (GraphPad, USA). $P < 0.05$ was considered to be statistical significance.

AUTHOR CONTRIBUTIONS

JX Y and JL L designed the research and oversaw the writing of the manuscript. P W and JJ S performed the experiments and wrote the manuscript, XH L and YM D analyzed the data. All authors have read and approved the manuscript.

CONFLICTS OF INTEREST

FUNDING

REFERENCES

1. Singh J, Vishwakarma K, Ramawat N, Rai P, Singh VK, Mishra RK, Kumar V, Tripathi DK, Sharma S. Nanomaterials and microbes' interactions: a contemporary overview. 3 Biotech. 2019; 9:68. https://doi.org/10.1007/s13205-019-1576-0 PMID:30729092

2. Teleanu DM, Chircov C, Grumezescu AM, Teleanu RI. Neurotoxicity of nanomaterials: an up-to-date overview. Nanomaterials (Basel). 2019; 9:96. https://doi.org/10.3390/nano9010096 PMID:30642104

3. Dhupal M, Oh JM, Tripathy DR, Kim SK, Koh SB, Park KS. Immunotoxicity of titanium dioxide nanoparticles via simultaneous induction of apoptosis and multiple toll-like receptors signaling through ROS-dependent SAPK/JNK and p38 MAPK activation. Int J Nanomedicine. 2018; 13:6735–50.

https://doi.org/10.2147/IJN.S176087
PMID:30425486

4. Fadoju O, Ogunsuyi O, Akanni O, Alabi O, Alimba C, Adaramoye O, Cambier S, Eswara S, Gutleb AC, Bakare A. Evaluation of cytogenotoxicity and oxidative stress parameters in male Swiss mice co-exposed to titanium dioxide and zinc oxide nanoparticles. Environ Toxicol Pharmacol. 2019; 70:103204.
https://doi.org/10.1016/j.etap.2019.103204
PMID:31200344

5. Rebleanu D, Gaidau C, Voicu G, Constantinescu CA, Mansilla Sánchez C, Rojas TC, Carvalho S, Calin M. The impact of photocatalytic Ag/TiO$_2$ and Ag/N-TiO$_2$ nanoparticles on human keratinocytes and epithelial lung cells. Toxicology. 2019; 416:30–43.
https://doi.org/10.1016/j.tox.2019.01.013
PMID:30711708

6. Jin CY, Zhu BS, Wang XF, Lu QH. Cytotoxicity of titanium dioxide nanoparticles in mouse fibroblast cells. Chem Res Toxicol. 2008; 21:1871–77.
https://doi.org/10.1021/tx800179f PMID:18680314

7. Gao X, Wang Y, Peng S, Yue B, Fan C, Chen W, Li X. Comparative toxicities of bismuth oxybromide and titanium dioxide exposure on human skin keratinocyte cells. Chemosphere. 2015; 135:83–93.
https://doi.org/10.1016/j.chemosphere.2015.03.075
PMID:25917605

8. Kansara K, Patel P, Shah D, Shukla RK, Singh S, Kumar A, Dhawan A. TiO2 nanoparticles induce DNA double strand breaks and cell cycle arrest in human alveolar cells. Environ Mol Mutagen. 2015; 56:204–17.
https://doi.org/10.1002/em.21925 PMID:25524809

9. Wu T, Tang M. The inflammatory response to silver and titanium dioxide nanoparticles in the central nervous system. Nanomedicine (Lond). 2018; 13:233–49.
https://doi.org/10.2217/nnm-2017-0270
PMID:29199887

10. Hong F, Yu X, Wu N, Zhang YQ. Progress of in vivo studies on the systemic toxicities induced by titanium dioxide nanoparticles. Toxicol Res (Camb). 2017; 6:115–33.
https://doi.org/10.1039/c6tx00338a PMID:30090482

11. Alvarez-Trabado J, López-García A, Martín-Pastor M, Diebold Y, Sanchez A. Sorbitan ester nanoparticles (SENS) as a novel topical ocular drug delivery system: design, optimization, and in vitro/ex vivo evaluation. Int J Pharm. 2018; 546:20–30.
https://doi.org/10.1016/j.ijpharm.2018.05.015
PMID:29753904

12. Kim S, Gates B, Leonard BC, Gragg M, Pinkerton KE, Winkle LV, Murphy CJ, Pyrgiotakis G, Zhang Z, Demokritou P, Thomasy SM. Engineered metal oxide nanomaterials inhibit corneal epithelial wound healing in vitro and in vivo. NanoImpact. 2020; 17:100198.
https://doi.org/10.1016/j.impact.2019.100198
PMID:32154443

13. De Matteis V, Rizzello L. Noble metals and soft bio-inspired nanoparticles in retinal diseases treatment: a perspective. Cells. 2020; 9:679.
https://doi.org/10.3390/cells9030679
PMID:32164376

14. Zhu S, Gong L, Li Y, Xu H, Gu Z, Zhao Y. Safety assessment of nanomaterials to eyes: an important but neglected issue. Adv Sci (Weinh). 2019; 6:1802289.
https://doi.org/10.1002/advs.201802289
PMID:31453052

15. Lee H, Park K. In vitro cytotoxicity of zinc oxide nanoparticles in cultured statens seruminstitut rabbit cornea cells. Toxicol Res. 2019; 35:287–94.
https://doi.org/10.5487/TR.2019.35.3.287
PMID:31341558

16. Chen X, Zhu S, Hu X, Sun D, Yang J, Yang C, Wu W, Li Y, Gu X, Li M, Liu B, Ge L, Gu Z, Xu H. Toxicity and mechanism of mesoporous silica nanoparticles in eyes. Nanoscale. 2020; 12:13637–53.
https://doi.org/10.1039/d0nr03208e PMID:32567638

17. Song B, Zhou T, Yang W, Liu J, Shao L. Contribution of oxidative stress to TiO$_2$ nanoparticle-induced toxicity. Environ Toxicol Pharmacol. 2016; 48:130–40.
https://doi.org/10.1016/j.etap.2016.10.013
PMID:27771506

18. Agban Y, Lian J, Prabakar S, Seyfoddin A, Rupenthal ID. Nanoparticle cross-linked collagen shields for sustained delivery of pilocarpine hydrochloride. Int J Pharm. 2016; 501:96–101.
https://doi.org/10.1016/j.ijpharm.2016.01.069
PMID:26828672

19. Wu Q, Guo D, Du Y, Liu D, Wang D, Bi H. UVB irradiation enhances TiO2 nanoparticle-induced disruption of calcium homeostasis in human lens epithelial cells. Photochem Photobiol. 2014; 90:1324–31.
https://doi.org/10.1111/php.12322 PMID:25059545

20. Thakur A, Alam MJ, Ajayakumar MR, Ghaskadbi S, Sharma M, Goswami SK. Norepinephrine-induced apoptotic and hypertrophic responses in H9c2 cardiac myoblasts are characterized by different repertoire of reactive oxygen species generation. Redox Biol. 2015; 5:243–52.
https://doi.org/10.1016/j.redox.2015.05.005
PMID:26070033

21. Yamamoto M, Kensler TW, Motohashi H. The KEAP1-NRF2 system: a thiol-based sensor-effector apparatus for maintaining redox homeostasis. Physiol Rev. 2018; 98:1169–203.

https://doi.org/10.1152/physrev.00023.2017
PMID:29717933

22. Grande F, Tucci P. Titanium dioxide nanoparticles: a risk for human health? Mini Rev Med Chem. 2016; 16:762–69.
https://doi.org/10.2174/1389557516666160321114341
PMID:26996620

23. He Q, Zhou X, Liu Y, Gou W, Cui J, Li Z, Wu Y, Zuo D. Titanium dioxide nanoparticles induce mouse hippocampal neuron apoptosis via oxidative stress- and calcium imbalance-mediated endoplasmic reticulum stress. Environ Toxicol Pharmacol. 2018; 63:6–15.
https://doi.org/10.1016/j.etap.2018.08.003
PMID:30114659

24. Lushchak VI. Environmentally induced oxidative stress in aquatic animals. Aquat Toxicol. 2011; 101:13–30.
https://doi.org/10.1016/j.aquatox.2010.10.006
PMID:21074869

25. Bardaweel SK, Gul M, Alzweiri M, Ishaqat A, ALSalamat HA, Bashatwah RM. Reactive oxygen species: the dual role in physiological and pathological conditions of the human body. Eurasian J Med. 2018; 50:193–201.
https://doi.org/10.5152/eurasianjmed.2018.17397
PMID:30515042

26. Tsikas D. Assessment of lipid peroxidation by measuring malondialdehyde (MDA) and relatives in biological samples: analytical and biological challenges. Anal Biochem. 2017; 524:13–30.
https://doi.org/10.1016/j.ab.2016.10.021
PMID:27789233

27. Bułdak RJ, Bułdak Ł, Kukla M, Gabriel A, Zwirska-Korczala K. Significance of selected antioxidant enzymes in cancer cell progression. Pol J Pathol. 2014; 65:167–75.
https://doi.org/10.5114/pjp.2014.45779
PMID:25372413

28. Zhang R, Niu Y, Li Y, Zhao C, Song B, Li Y, Zhou Y. Acute toxicity study of the interaction between titanium dioxide nanoparticles and lead acetate in mice. Environ Toxicol Pharmacol. 2010; 30:52–60.
https://doi.org/10.1016/j.etap.2010.03.015
PMID:21787629

29. Abbasi-Oshaghi E, Mirzaei F, Pourjafar M. NLRP3 inflammasome, oxidative stress, and apoptosis induced in the intestine and liver of rats treated with titanium dioxide nanoparticles: in vivo and in vitro study. Int J Nanomedicine. 2019; 14:1919–36.
https://doi.org/10.2147/IJN.S192382
PMID:30936694

30. Cadet J, Davies KJ. Oxidative DNA damage & repair: an introduction. Free Radic Biol Med. 2017; 107:2–12.
https://doi.org/10.1016/j.freeradbiomed.2017.03.030
PMID:28363603

31. Heijink AM, Krajewska M, van Vugt MA. The DNA damage response during mitosis. Mutat Res. 2013; 750:45–55.
https://doi.org/10.1016/j.mrfmmm.2013.07.003
PMID:23880065

32. Zhang C, Peng G. Non-coding RNAs: an emerging player in DNA damage response. Mutat Res Rev Mutat Res. 2015; 763:202–11.
https://doi.org/10.1016/j.mrrev.2014.11.003
PMID:25795121

33. Hong F, Wu N, Ge Y, Zhou Y, Shen T, Qiang Q, Zhang Q, Chen M, Wang Y, Wang L, Hong J. Nanosized titanium dioxide resulted in the activation of TGF-β/smads/p38MAPK pathway in renal inflammation and fibration of mice. J Biomed Mater Res A. 2016; 104:1452–61.
https://doi.org/10.1002/jbm.a.35678
PMID:26850371

34. Kim H, Jeon D, Oh S, Nam K, Son S, Gye MC, Shin I. Titanium dioxide nanoparticles induce apoptosis by interfering with EGFR signaling in human breast cancer cells. Environ Res. 2019; 175:117–23.
https://doi.org/10.1016/j.envres.2019.05.001
PMID:31112848

35. Lee H, Choi YK. Regenerative effects of heme oxygenase metabolites on neuroinflammatory diseases. Int J Mol Sci. 2018; 20:78.
https://doi.org/10.3390/ijms20010078
PMID:30585210

36. Liu C, Chen Y, Kochevar IE, Jurkunas UV. Decreased DJ-1 leads to impaired Nrf2-regulated antioxidant defense and increased UV-a-induced apoptosis in corneal endothelial cells. Invest Ophthalmol Vis Sci. 2014; 55:5551–60.
https://doi.org/10.1167/iovs.14-14580
PMID:25082883

37. Zheng X, Cui H, Yin Y, Zhang Y, Zong R, Bao X, Ma JX, Liu Z, Zhou Y. SERPINA3K ameliorates the corneal oxidative injury induced by 4-hydroxynonenal. Invest Ophthalmol Vis Sci. 2017; 58:2874–83.
https://doi.org/10.1167/iovs.17-21544
PMID:28586911

38. Chidiac R, Zhang Y, Tessier S, Faubert D, Delisle C, Gratton JP. Comparative phosphoproteomics analysis of VEGF and angiopoietin-1 signaling reveals ZO-1 as a critical regulator of endothelial cell proliferation. Mol Cell Proteomics. 2016; 15:1511–25.
https://doi.org/10.1074/mcp.M115.053298
PMID:26846344

39. Matchkov VV, Krivoi II. Specialized functional diversity and interactions of the Na, K-ATPase. Front Physiol. 2016; 7:179.

https://doi.org/10.3389/fphys.2016.00179
PMID:27252653

40. Okumura N, Nakamura T, Kay EP, Nakahara M, Kinoshita S, Koizumi N. R-spondin1 regulates cell proliferation of corneal endothelial cells via the Wnt3a/β-catenin pathway. Invest Ophthalmol Vis Sci. 2014; 55:6861–69.
https://doi.org/10.1167/iovs.14-14091
PMID:25277232

41. Hong F, Ze Y, Zhou Y, Hong J, Yu X, Sheng L, Wang L. Nanoparticulate TiO_2-mediated inhibition of the Wnt signaling pathway causes dendritic development disorder in cultured rat hippocampal neurons. J Biomed Mater Res A. 2017; 105:2139–49.
https://doi.org/10.1002/jbm.a.36073 PMID:28371053

42. An W, Zhang Y, Zhang X, Li K, Kang Y, Akhtar S, Sha X, Gao L. Ocular toxicity of reduced graphene oxide or graphene oxide exposure in mouse eyes. Exp Eye Res. 2018; 174:59–69.
https://doi.org/10.1016/j.exer.2018.05.024
PMID:29803558

43. Lu X, Chen Z, Mylarapu N, Watsky MA. Effects of 1,25 and 24,25 vitamin D on corneal epithelial proliferation, migration and vitamin D metabolizing and catabolizing enzymes. Sci Rep. 2017; 7:16951.
https://doi.org/10.1038/s41598-017-16698-3
PMID:29208972